JOURNAL OF COMPUTATIONAL PHYSICS 59, 81–95 (1985)

Accurate Solution of Three-Dimensional Poisson's Equation in Cylindrical Coordinate by Expansion in Chebyshev Polynomials

C. S. TAN

Gas Turbine & Plasma Dynamics Laboratory, Department of Aeronautics and Astronautics, Massachusetts Institute of Technology, Cambridge, Massachusetts 02139

Received July 21, 1983; revised March 20, 1984

I. INTRODUCTION

In recent years Gottlieb and Orszag [1, 2] have shown that for smooth solutions (i.e., infinitely differentiable functions) of differential equations, high accuracy can be attained using spectral methods. In these methods, the solution being sought is approximated by a (truncated) series of smooth basic functions and the exponential convergence of the series is obtained if these basic functions are suitably chosen; for example, Fourier series should be used for problems with periodic boundary conditions while eigenfunctions such as Chebyshev and Legendre polynomials of the singular Sturm–Liouville problem should be chosen for problems with the general type of boundary conditions [1].

Spectrally accurate solution of Poisson's equation in a square with homogeneous Dirichlet boundary conditions by expansion in Chebyshev polynomials have been obtained by Haidvogel and Zang [3]. Deville [4] has further extended the spectral solution of Poisson's equation in a rectangular domain with general type of boundary conditions.

In this note, a spectrally accurate solution for three-dimensional Poisson's equation and Helmholtz's equation using Chebyshev series and Fourier series is described for a simple domain in a cylindrical coordinate system. The boundary conditions imposed can be either homogeneous or inhomogeneous and of Dirichlet, Neumann, or general mixed type. In particular, such domain could be a bend of rectangular cross section as shown in Fig. 1. It will also be shown that a mixed-spectral-finite-difference approach to the solution of the Poisson's equation and Helmholtz's equation in such a domain can readily be implemented as well.

II. MATHEMATICAL FORMULATION

The right-handed cylindrical coordinate system (r, θ, z) (Fig. 1) will be used.

We nondimensionalize the length in such a way that (e.g., for a bend, lengths are then in units of half the height of the bend)

$$-1 \leqslant Z \leqslant 1;$$

0021-9991/85 $3.00

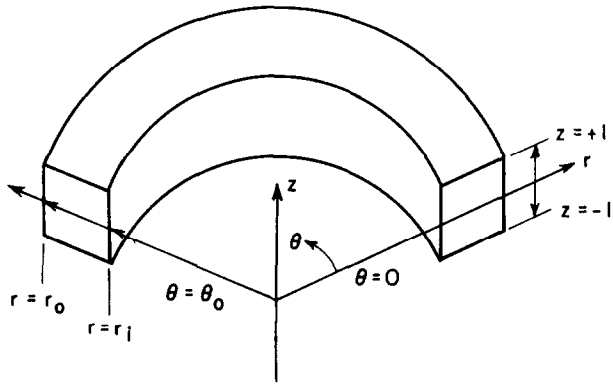

FIG. 1. A bend of rectangular cross section in cylindrical coordinate system (r, θ, Z).

r_i and r_o are the inner and outer radius, and the azimuthal coordinate θ extends from 0 to θ_0, i.e.,

$$0 \leqslant \theta \leqslant \theta_0.$$

Before expanding the solution $U(r, \theta, Z)$ in a series of Chebyshev polynomials, the domain in (r, θ, Z),

$$r_i \leqslant r \leqslant r_o;$$
$$0 \leqslant \theta \leqslant \theta_o;$$
$$-1 \leqslant Z \leqslant 1;$$

is mapped into the domain in (R, ϕ, Z) such that

$$-1 \leqslant R \leqslant 1;$$
$$-1 \leqslant \phi \leqslant 1;$$
$$-1 \leqslant Z \leqslant 1;$$

using

$$r = \eta R + \xi \tag{2.1a}$$

and

$$\theta = \tfrac{1}{2}(1 + \phi)\,\theta_0 \tag{2.1b}$$

where $\eta = \frac{1}{2}(r_o - r_i)$, $\xi = \frac{1}{2}(r_o + r_i)$.

In (R, ϕ, Z), the Poisson's equation and the Helmholtz's equation can be written as

$$\left(\mathscr{L} + \frac{4}{(\eta R + \xi)^2}\frac{1}{\theta_0^2}\frac{\partial^2}{\partial \phi^2} + \frac{\partial^2}{\partial Z^2}\right) U(R, \phi, Z) = S(R, \phi, Z), \tag{2.2}$$

where the differential operator $\mathscr{L}$ is given by

$$\mathscr{L} = \frac{1}{\eta^2}\frac{\partial^2}{\partial R^2} + \frac{1}{\eta(\eta R + \xi)}\frac{\partial}{\partial R} \tag{2.3}$$

for Poisson's equation, and

$$\mathscr{L} = \frac{1}{\eta^2}\frac{\partial^2}{\partial R^2} + \frac{1}{\eta(\eta R + \xi)}\frac{\partial}{\partial R} + \frac{K_1}{(\eta R + \xi)^2} + K_0 \tag{2.4}$$

(both K_0 and K_1 are constants) for Helmoltz's equation.

The boundary conditions can be of the general type as follows.

$$\text{at} \quad R = \pm 1: \qquad \alpha_\pm U(\phi, Z) + \beta_\pm \frac{\partial U}{\partial R} = F_\pm(\phi, Z) \tag{2.5a, b}$$

$$\text{at} \quad \phi = \pm 1: \qquad a_\pm U(R, Z) + b_\pm \frac{\partial U}{\partial \phi} = G_\pm(R, Z) \tag{2.5c, d}$$

$$\text{at} \quad Z = \pm 1: \qquad A_\pm U(R, \phi) + B_\pm \frac{\partial U}{\partial Z} = H_\pm(R, \phi) \tag{2.5e, f}$$

In Eq. (2.5), the subscript + pertains to that at $R, \phi, Z = +1$ while the subscript − pertains to that at $R, \phi, Z = -1$.

In the spectral approach to the solution of Eq. (2.2) using Chebyshev polynomials, all the functions U, S, $F_\pm$, $G_\pm$, and $H_\pm$ are approximated by truncated Chebyshev series as follows:

$$\begin{Bmatrix} U(R, \phi, Z) \\ S(R, \phi, Z) \\ F_\pm(\phi, Z) \end{Bmatrix} = \sum_{m=0}^{M} \sum_{n=0}^{N} \begin{Bmatrix} U_{mn}(R) \\ S_{mn}(R) \\ f_{\pm mn} \end{Bmatrix} T_m(\phi)\, T_n(Z) \tag{2.6a, b, c}$$

$$G_\pm(R, Z) = \sum_{n=0}^{N} g_{\pm n}(R)\, T_n(Z) \tag{2.6d}$$

$$H_\pm(R, \phi) = \sum_{m=0}^{M} h_{\pm m}(R)\, T_m(\phi) \tag{2.6e}$$

The R-dependence in Eq. (2.6) is kept with the intention of using the collocation approximation over the Chebyshev grid points in the radial coordinate. However, if desired, $U_{mn}(R)$, $S_{mn}(R)$, $g_{\pm n}(R)$, and $h_{\pm m}(R)$ can be written as

$$\begin{Bmatrix} U_{mn}(R) \\ S_{mn}(R) \\ g_{\pm n}(R) \\ h_{\pm m}(R) \end{Bmatrix} = \sum_{l=0}^{L} \begin{Bmatrix} U_{lmn} \\ S_{lmn} \\ g_{\pm ln} \\ h_{\pm lm} \end{Bmatrix} T_l(R). \tag{2.7a, b, c, d}$$

In the expressions in (2.6) to (2.7) the Chebyshev polynomials $T_l(R)$ can be expressed as

$$T_l(R) = \cos(l \cos^{-1} R). \tag{2.8}$$

By taking the Chebyshev-tau approximation approach in the ϕ and Z, we can make use of the recurrence relations for the derivatives of Chebyshev polynomials [1] and the boundary conditions (2.5c, d) to (2.5e, f) to write

$$\begin{Bmatrix} \dfrac{\partial^2 U}{\partial^2 \phi} \\ \dfrac{\partial^2 U}{\partial Z^2} \end{Bmatrix} = \sum_{m=0}^{M} \sum_{n=0}^{N} \begin{Bmatrix} U_{mn}^{(2,0)}(R) \\ U_{mn}^{(0,2)}(R) \end{Bmatrix} T_m(\phi)\, T_n(Z) \tag{2.9}$$

$$U_{mn}^{(2,0)}(R) = \sum_{p=0}^{M-2} C_{mp} U_{pn}(R) + B_{mn}(R) \tag{2.10}$$

and

$$U_{mn}^{(0,2)}(R) = \sum_{q=0}^{N-2} \gamma_{nq} U_{mq}(R) + D_{mn}(R) \tag{2.11}$$

where the C_{mp} and the boundary term $B_{mn}(R)$ are given in Eqs. (A.1) to (A.4) in the Appendix, the γ_{nq} and the boundary term $D_{mn}(R)$ are given in Eqs. (A.6) to (A.9) in the Appendix.

Substitution of Eq. (2.11) and (2.12) in (2.2), together with the use of Eqs. (2.6a) and (2.6b), yields

$$\mathscr{L} U_{mn}(R) + \frac{4}{\theta_0^2(\eta R + \xi)^2} \sum_{p=0}^{M-2} C_{mp} U_{pn}(R) + \sum_{q=0}^{N-2} \gamma_{nq} U_{mq}(R) = \sigma_{mn}(R), \tag{2.12a}$$

where

$$\sigma_{mn}(R) = S_{mn}(R) - \frac{4}{\theta_0^2(\eta R + \xi)^2} B_{mn}(R) - D_{mn}(R). \tag{2.12b}$$

The original three-dimensional equation (2.2) has now been reduced to a system of coupled one-dimensional differential equations with the m and n in Eq. (2.13) running from 0 to $(M-2)$ and from 0 to $(N-2)$, respectively.

Note that had the boundary conditions at $\phi = \pm 1$ and $Z = \pm 1$ been of the homogeneous type, then the terms involving $B_{mn}(R)$ and $D_{mn}(R)$ on the r.h.s. of Eq. (2.13) would be identically zero. Such a technique of handling the general inhomogeneous boundary conditions encountered in the solution of the elliptic equation was pointed out by Deville [4].

If a second-order differencing is used over a uniform grid lines of spacing $\Delta\theta$ in the θ-direction, then Eq. (2.2) simply reduces to

$$\left(\mathscr{L}+\frac{\partial^2}{\partial Z^2}\right)U_j+\frac{1}{(\eta R+\xi)^2(\Delta\theta)^2}(U_{j-1}-2U_j+U_{j+1})=S(R, j\,\Delta\theta, Z) \quad (2.14)$$

where mapping is only done in the radial direction only; $\Delta\theta=\theta_0/M$ and $j=0, 1, 2,..., M-1, M$. The imposition of boundary conditions at $\theta=0$ and θ_0 is standard.

For periodic boundary conditions in the θ-direction Fourier series should be used (in the θ-direction) by writing $U(R, \theta, Z)$ as

$$U(R, \theta, Z)=\sum_{m=-M/2}^{M/2-1}\sum_{n=0}^{N}U_{mn}(R)\,e^{im2\pi\theta/\theta_0}T_n(Z), \quad (2.15)$$

where $U_{mn}(R)$ can also be written in the form given in Eq. (2.7a).

Both U_{mn} and U_{lmn} are the Chebyshev–Fourier coefficients. The case of $\theta_0=2\pi$ corresponds to an annular geometry (Fig. 2) that is typical of flow in turbomachines where periodicity in the radial and axial direction is not usually valid. In this particular case, $U_{mn}(R)$ should be calculated from

$$\left[\mathscr{L}-\frac{(2\pi m/\theta_0)^2}{(\eta R+\xi)^2}\right]U_{mn}(R)+\sum_{q=0}^{N-2}\gamma_{nq}U_{mq}(R)=S_{mn}(R)-D_{mn}(R) \quad (2.16)$$

for $m=-M/2$ to $M/2-1$.

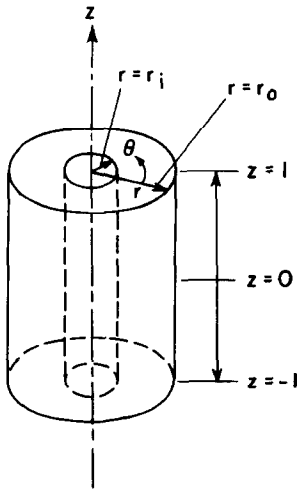

FIG. 2. A cylindrical annulus of constant inner and outer radius.

III. Numerical Methods

We now diagonalize the matrix C of dimension $(M-1)$ by $(M-1)$ with elements C_{mp} and the matrix Γ of dimension $(N-1)$ by $(N-1)$ with elements γ_{nq} as

$$E^{-1}CE = \Lambda \tag{3.1}$$

and

$$\varepsilon^{-1}\Gamma\varepsilon = \chi \tag{3.2}$$

where Λ is a diagonal matrix of dimension $(M-1)$ with diagonal elements λ_m as eigenvalues of the matrix C, χ is a diagonal matrix of dimension $(N-1)$ with diagonal elements χ_n as eigenvalues of the matrix Γ, the matrices E and ε are the corresponding eigenvector matrices.

In addition, given the matrices U and σ which are of dimension $(M-1)$ by $(N-1)$ with elements $U_{mn}(R)$ and $\sigma_{mn}(R)$, one can obtain corresponding matrices $\hat{U}$ with elements $\hat{U}_{mn}(R)$ and $\hat{\sigma}$ with element $\hat{\sigma}_{mn}(R)$ from

$$U = E\hat{U}\varepsilon^{T} \tag{3.3}$$

$$\sigma = E\hat{\sigma}\varepsilon^{T} \tag{3.4}$$

where the superscript T denotes the transpose of the matrix.

Use of Eqs. (3.1) to (3.4) in Eq. (2.13) yields

$$\left[\mathscr{L} + \frac{4}{\theta_0^2\eta^2(R+\xi/\eta)^2}\lambda_m + \chi_n\right]\hat{U}_{mn}(R) = \hat{\sigma}_{mn}(R). \tag{3.5}$$

This process effectively decouples the system of one-dimensional equations in (2.13) thus permitting the solution of $\hat{U}_{mn}(R)$ for each m and n as described below.

III.A *Method of Collocation followed by Diagonalisation*

The collocation approximation $\mathscr{L}_c$ to the differential operator $\mathscr{L}$ is given by

$$[\mathscr{L}_c\hat{U}_{mn}]_{R=R_i} = \sum_{l=0}^{L} L_{il}\hat{U}_{mn}(R_l) \tag{3.6}$$

where

$$L_{il} = \frac{1}{\eta^2}d_{il}^{*(2)} + \frac{1}{\eta(\eta R_i+\xi)}d_{il}^{*(1)} + \frac{K_1}{(\eta R+\xi)^2}. \tag{3.7}$$

In Eq. (3.7), $d_{il}^{*(2)}$ and $d_{il}^{*(1)}$ are, respectively, the elements of the collocation approximation to the second-order differential operator d^2/dR^2 and the first-order

differential operator d/dR over the Chebychev points $R_i = \cos \pi i/L$ [5, 6]. The boundary conditions at $R = \pm 1$ gives

$$\hat{U}_{mn}(-1) = \sum_{i=1}^{L-1} Q_i \hat{U}_{mn}(R_i) + \hat{V}_{mn} \tag{3.8a}$$

$$\hat{U}_{mn}(+1) = \sum_{i=1}^{L-1} P_i \hat{U}_{mn}(R_i) + \hat{T}_{mn} \tag{3.8b}$$

where P_i, $\hat{T}_{mn}$, Q_i, and $\hat{V}_{mn}$ are given in Eq. (A.11) in the Appendix. The boundary terms $\hat{T}_{mn}$ and $\hat{V}_{mn}$ are identically zero for homogeneous boundary conditions at $R = \pm 1$. The boundary conditions at $R = \pm 1$ are imposed by eliminating $\hat{U}_{mn}(-1)$ and $\hat{U}_{mn}(+1)$ from (3.6) so that

$$[\mathscr{L}_c \hat{U}_{mn}]_{R=R_i} = \sum_{l=1}^{L-1} L^*_{il} \hat{U}_{mn}(R_l) + \hat{Y}_{imn} \tag{3.9}$$

for $1 \leqslant i \leqslant L-1$, $1 \leqslant l \leqslant L-1$, where

$$L^*_{il} = L_{il} + L_{i0} P_l + L_{iL} Q_l \tag{3.10}$$

and

$$\hat{Y}_{imn} = L_{i0} \hat{T}_{mn} + L_{iL} \hat{V}_{mn}. \tag{3.11}$$

The collocation approximation to (3.5) can now be written as

$$[W^*_m + \chi]\, \hat{U}^*_R = \hat{\sigma}^*_R \tag{3.12}$$

where W^*_m is a collocation matrix of dimensions $(L-1)$ by $(L-1)$ with elements

$$w^*_{il} = L^*_{il} + \frac{4\lambda_m}{\theta_0^2(\eta R_i + \xi)^2} \tag{3.13}$$

for $1 \leqslant i \leqslant L-1$, $1 \leqslant l \leqslant L-1$; $\hat{U}^*_R$ is a column vector of length $(L-1)$ with elements $\hat{U}_{mn}(R_l)$ for $l = 1$ to $L-1$; and $\hat{\sigma}^*_R$ is a column vector of length $(L-1)$ with elements $\hat{\sigma}_{mn}(R_i) - \hat{Y}_{imn}$.

One can further proceed to diagonalise the collocation matrix W^*_m by [7]

$$\psi_m^{-1} W^*_m \psi_m = \Phi_m \tag{3.14}$$

where Φ_m is a diagonal matrix with diagonal elements ϕ_{ml} as the eigenvalues while ψ_m is the corresponding eigenvector matrix. This would be desirable for repeated solutions for $U(R, \phi, Z)$ with many different $S(R, \phi, Z)$.

The solution $\hat{U}^*_R$ for each m is given by

$$\hat{U}^*_R = \psi_m [\Phi_m + \chi]^{-1} \psi_m^{-1} \hat{\sigma}^*_R. \tag{3.15}$$

Once $\hat{U}_R^*$ is known, $\hat{U}_{mn}(-1)$ and $\hat{U}_{mn}(+1)$ can be obtained from Eq. (3.8). Equation (3.3) is then used to calculate $U_{mn}(R_i)$ for $m=0$ to $(M-2)$ and $n=0$ to $(N-2)$. Finally, $U_{M-1,n}(R_i)$, $U_{Mn}(R_i)$, $U_{m,N-1}(R_i)$, and $U_{m,N}(R_i)$ are calculated using the boundary conditions in Eqs. (2.5c, d) and (2.5e, f).

III.B *Spectral Iteration Method*

Following Orszag [2], we construct a spectral collocation approximation M_{sp} as well as a corresponding second-order finite difference approximation M_{ap} to the variable coefficient Chebyshev operator $[\mathscr{L}+(4/\theta_0^2(\eta R+\xi)^2)\lambda_m+\chi_n]$ at the Chebyshev grid lines given by $R_i=\cos \pi i/L$, taking proper account of the boundary conditions at $R=\pm 1$. Numerical calculations are implementd to estimate the upper and the lower bound of $\|M_{ap}^{-1}M_{sp}\|$; it is found that with $L=16$,

$$0\leqslant \mu_{\min} 0\leqslant \|M_{ap}^{-1}M_{ap}\|\leqslant \mu_{\max}<2.5 \tag{3.16}$$

for the relevant values of λ_m and χ_n encountered here. The $\hat{U}_{mn}(R_i)$ for $i=0$ to L are then obtained iteratively using Richardson (Jacobi) method,

$$M_{ap}\,\delta\hat{U}_R^{(\nu+1)}=-\omega(M_{sp}\,\hat{U}_R^{(\nu)}-\hat{\sigma}_R) \tag{3.17a}$$

$$\hat{U}_R^{(\nu+1)}=\hat{U}_R^{(\nu)}+\delta\hat{U}_R^{(\nu+1)} \tag{3.17b}$$

where the optimum value for ω is given by [2]

$$\omega=\frac{2}{\mu_{\min}+\mu_{\max}}. \tag{3.18}$$

The matrix M_{ap} is tridiagonal so that $O(L)$ operations are necessary to obtain $\delta\hat{U}_R$. $M_{sp}\hat{U}_R$ on the r.h.s. of Eq. (3.17a) can be evaluated efficiently using the FFT algorithm [8] in $O(L\log L)$ operations. The boundary conditions at $R=\pm 1$ are enforced by replacing the first and the last element of the r.h.s. of (3.17a) by

$$\left\{\left[\alpha_+\,\hat{U}_{mn}(R)+\beta_+\frac{d}{dR}\,\hat{U}_{mn}(R)\right]_{R=1}-\hat{f}_{+mn}\right\}$$

and

$$\left\{\left[\alpha_-\,\hat{U}_{mn}(R)+\beta_-\frac{d}{dR}\,\hat{U}_{mn}(R)\right]_{R=-1}-\hat{f}_{-mn}\right\},$$

respectively.

When the solution converges, i.e.,

$$\delta\hat{U}_R\to 0,$$

Eq. (3.4) and the boundary conditions will be satisfied exactly.

As in Section (III.A), the knowledge of $\hat{U}_{mn}(R)$ allows the determination of $U_{mn}(R)$ from Eq. (3.3) whence $U_{M-1,n}$, $U_{M,n}$, $U_{m,N-1}$, and $U_{m,N}$ can be determined using the boundary conditions in Eqs. (2.5c, d) and (2.5e, f).

Finally, if a mixed-spectral-finite difference method with second-order differencing over a uniform grid lines of spacing $\Delta\theta$ in the θ-direction is used, the matrix C simply becomes a tridiagonal matrix with off-diagonal elements $1/(\Delta\theta)^2$ and diagonal elements $-2/(\Delta\theta)^2$. Apart from this, the solution technique is the same as described above. Similarly if periodicity holds in the θ-direction, the matrix C simply becomes a diagonal matrix with elements $-(2\pi m/\theta_0)^2$ for $m=-M/2$ to $(M/2)-1$, where m is the wave number. In this case, $U(R, \theta, Z)$ is simply given by Eq. (2.15). Note that when $\theta_0=2\pi$, the domain becomes an annular one (Fig. 2).

IV. Results

We have developed computer programs for solving the three-dimensional Poisson and Helmholtz's equations in cylindrical coordinate by (i) an expansion in a triple series of Chebyshev polynomials, (ii) a mixed-spectral finite difference technique, and (iii) an expansion in a Chebyshev–Fourier series whenever periodicity in the θ-direction is applicable. We choose $(R_i, \phi_j, Z_k)=(\cos \pi i/L, \cos \pi j/M, \cos \pi k/N)$ so that the truncated Chebyshev series are mere discrete cosine series, and for values of L, M, and N which are power of 2, the FFT algorithm [8] can be used efficiently for the evaluation and the inversion of these series.

For illustrating the accuracy and the convergence character of the different solution procedures, the double precision version of the computer programs were used for obtaining numerical solutions to Eq. (2.2). The function $S(r, \theta, Z)$ on the r.h.s. of Eq. (2.2) has been chosen so that an analytical solution $U(r, \theta, Z)$ can be obtained with different types of imposed boundary conditions. For the case of a three-dimensional Poisson's equation, $S(r, \theta, Z)$ is chosen so that the analytical solution $U(r, \theta, Z)$ is

$$U(r,\theta,Z)=\left[\cos\left\{\frac{\pi}{2}\left[\frac{1}{\eta}(r-\xi)-1.0\right]\right\}+\sin\left\{\frac{\pi}{2}\left[\frac{1}{\eta}(r-\xi)-1.0\right]\right\}\right]$$
$$\times\left[\cos\left\{\pi\left(\frac{\theta}{\theta_0}-1\right)\right\}+\sin\left\{\pi\left(\frac{\theta}{\theta_0}-1\right)\right\}\right]\left[\cos\left\{\frac{\pi}{2}(Z-1)\right\}+\sin\left\{\frac{\pi}{2}(Z-1)\right\}\right] \tag{4.1}$$

with $r_i=2$, $r_0=4$, $\theta_0=0.5$.

The computer codes were run on the DEC PDP 11/70 as well as Perkin–Elmer 3242 minicomputers. To elucidate the features and accuracy of the method, different types of boundary conditions and different resolution ranging from 4 by 4 by 4 to 32 by 32 by 32 are used. By evaluating $U(r, \theta, Z)$ on the boundaries and by choosing various combinations of boundary constants, $\alpha_\pm$, $\beta_\pm$, $a_\pm$, $b_\pm$, $A_\pm$, and $B_\pm$,

different types of boundary conditions may be imposed to obtain the numerical solution. Table I shows the results obtained spectrally using a triple series of Chebyshev polynomials. In Table I, with the exception of the last one all cases have been done with boundary constants $\alpha_{\pm}$, $\beta_{\pm}$, $a_{\pm}$, $b_{\pm}$, $A_{\pm}$, and $B_{\pm}$ taken to be 0 or one. For the last case in Table I, we have taken $r_1 = 5.0$, $r_0 = 10.0$, $\theta_0 = 1.5707963$ (corresponding to a bend of 90°),

$$\alpha_+ = 1.5, \quad \beta_+ = 3.25, \quad \alpha_- = 0.5, \quad \beta_- = 1.45,$$
$$a_+ = 2.75, \quad b_+ = -1.95, \quad a_- = 5.0, \quad b_- = 7.15,$$
$$A_+ = -1.85, \quad B_+ = 10.0, \quad A_- = 25.0, \quad B_- = -70.$$

The representative timings shown in Table I and in subsequent tables pertain to the Perkin–Elmer 3242 minicomputer. The results in Table I show that for the various type of boundary conditions used, the maximum pointwise error between the numerical solution and the exact analytical solution is of the order of 10^{-10} for a resolution of 16 by 16 by 16. These results show the proper treatment of boundary conditions (homogeneous or inhomogeneous). Since the mathematical features of spectral methods follow very closely those of the partial differential equation being solved, an *incorrect treatment* of the *boundary conditions* will yield the *erroneous solution.*

Table II shows the accuracy attained for the resolution ranging from 4 by 4 by 4 to 32 by 32 by 32. The observed rapid convergence is representative of the perfor-

TABLE I

Use of Different Types of Boundary Conditions[a]

Type of boundary conditions	Resolution	Maximum pointwise error	CPU time for execution (sec)	CPU time for preprocessing sec
Dirichlet on all boundaries	$16 \times 16 \times 16$	$1.9987056 \times 10^{-10}$	26.634	12.398
Neumann in R Dirichlet in ϕ and Z	$16 \times 16 \times 16$	1.863627×10^{-10}	26.721	12.853
Mixed type in R Neumann in ϕ Dirichlet in Z	$16 \times 16 \times 16$	1.874447×10^{-10}	26.618	12.826
Mixed type in R & ϕ Neumann in Z	$16 \times 16 \times 16$	1.988369×10^{-10}	26.766	13.182
Mixed type on all boundaries	$16 \times 16 \times 16$	3.356077×10^{-10}	26.640	13.083
Mixed type on all boundaries	$16 \times 16 \times 16$	$2.0958088 \times 10^{-10}$	26.606	13.095

[a] Given CPU time on PE-3242 mini-computer only.

TABLE II

Accuracy versus Resolution[a]

Resolution	Maximum pointwise error	CPU time for execution (min: sec)	CPU time for preprocessing (min: sec)
$4\times4\times4$	0.113464	0.399	0.167
$8\times8\times8$	9.53562×10^{-6}	2.259	1.142
$16\times16\times16$	1.874447×10^{-10}	26.618	12.826
$32\times32\times32$	$6.015223874\times10^{-10}$	9:41.830	2:43.699

[a] Boundary conditions: mixed type at $R=\pm1$, Neumann at $\phi=\pm1$, Dirichlet at $z=\pm1$. Given CPU time on PE-3242 mini-computer only.

mance of the Chebyshev expansion for solutions which are infinitely differentiable.

For the case where $\mathscr{L}$ is that given in Eq. (2.4), we take $K_0=10$ and $K_1=15$. The corresponding $S(r,\theta,Z)$ is obtained by substituting for $U(r,\theta,Z)$ from Eq. (4.1) into Eq. (2.2). With a resolution of 16 by 16 by 16, the maximum pointwise error between the numerical solution and the exact analytical solution is 1.882379×10^{-10}. For this case, the boundary conditions used were of the mixed type at $R=\pm1$, the Neumann type at $\phi=\pm1$, and the Dirichlet type at $Z=\pm1$.

Table III shows the results on the maximum pointwise error obtained if a second-order-finite difference is used over a uniform grid in the θ-direction. The test function is again that given in Eq. (4.1) and Dirichlet boundary condition is applied on all boundaries. The accuracy of spectral solution is superior to that of mixed-spectral-finite-difference scheme. The mixed-spectral-finite-difference scheme has been tested with a second-order polynomial in θ (e.g., $a0+a1\theta+a2\theta^2$, where $a0$, $a1$ and $a2$ are given constants) replacing the $\cos[\pi(\theta/\theta_0-1)]+\sin[\pi(\theta/\theta_0-1)]$ in Eq. (4.1), and the resulting maximum pointwise error is of the order of 10^{-11} with any boundary conditions for a resolution of 16 by 19 by 16. Thus, if variation of U in the θ-direction is gradual and approximates that of a low-order polynomial, the

TABLE III[a]

Resolution	Maximum pointwise error	CPU time for execution (min: sec)	CPU tim for preprocessing (min: sec)
$8\times8\times8$	1.2640248×10^{-2}		
$16\times16\times16$	3.16270205×10^{-3}	27.003	14.190
$16\times20\times16$	2.247064×10^{-3}		
$16\times32\times16$	7.936344×10^{-4}	55.622	51.319
$32\times32\times32$	8.02785×10^{-4}	10:14.026	2:49.145
$16\times64\times16$	1.9841793×10^{-4}	2:03.836	1:30.782

[a] Given CPU time on PE-3242 mini-computer only.

TABLE IV[a]

Resolution	Maximum pointwise error
$8\times8\times8$	7.574855×10^{-6}
$16\times16\times16$	1.401398×10^{-10}

[a] Boundary conditions: mixed type at $R=\pm1$, $Z=\pm1$, periodic in θ-direction.

use of a second-order finite difference over a uniform grid in the θ-direction is justified.

In the case where periodicity is applicable in the θ-direction the maximum pointwise error obtained for a test function given by

$$U(r,\theta,Z)=\left[\cos\left\{\frac{\pi}{2}\left[\frac{1}{\eta}(r-\xi)-1.0\right]\right\}+\sin\left\{\frac{\pi}{2}\left[\frac{1}{\eta}(r-\xi)-1.0\right]\right\}\right]\left[\cos\left(\frac{2\pi\theta}{\theta_0}-1\right)+\sin\left(\frac{2\pi\theta}{\theta_0}-1\right)\right]\left[\cos\left\{\frac{\pi}{2}(Z-1)\right\}+\sin\left\{\frac{\pi}{2}(Z-1)\right\}\right] \tag{4.2}$$

is shown in Table IV.

Finally, the technique of spectral iteration described in Section (III.B) is used to solve the Poisson's equation with U expanded as a triple Chebyshev series. As before, the test function is that given in Eq. (4.1). For a resolution of $16\times16\times16$ after some 34 iterations the maximum pointwise error reduces to 2.82928×10^{-10}; Dirichlet boundary conditions are imposed on all boundaries. In general, the use of spectral iteration technique may need more CPU time than the use of a direct method that applies matrix diagonalization to all the differential operators. However, it should be noted that a simple Richardson iteration technique has been used here; the CPU time could further be reduced by employing acceleration methods.

Appendix

The C_{mp} and the $B_{mn}(R)$ in Eq. (2.11) are given as follows: for odd m with all p such that $0\leqslant p\leqslant m+1$ and with even p such that $m+3\leqslant p\leqslant M-2$

$$C_{mp}=\frac{1}{D_{ab}C_m}(M-1)[(M-1)^2-m^2]\{(a_--b_-M^2)(a_++b_+p^2)-(a_++b_+M^2)(-1)^p(a_--b_-p^2)\} \tag{A.1a}$$

while with odd p such that $m+2\leqslant p\leqslant M-3$

$$C_{mp}=\frac{1}{C_m}p(p^2-m^2)+\frac{1}{D_{ab}C_m}(M-1)[(M-1)^2-m^2]\{(a_--b_-M^2)(a_++b_+p^2)-(a_++b_+M^2)(-1)^p(a_--b_-p^2). \tag{A.1b}$$

$B_{mn}(R)$ is the boundary term given by

$$B_{mn}(R)=\frac{1}{D_{ab}C_m}(M-1)[(M-1)^2-m^2]$$
$$\times\{[a_+ + b_+ M^2]\, g_{-n} - [a_- - b_- M^2]\, g_{+n}\}; \tag{A.2}$$

and for even m with all p such that $0 \leqslant p \leqslant m+1$ and with odd p such that $m+3 \leqslant p \leqslant M-2$

$$C_{mp}=\frac{1}{D_{ab}C_m}M(M^2-m^2)\{[a_- - b_-(M-1)^2][a_+ + b_+ p^2]$$
$$+ [a_+ + b_+(M-1)^2](-1)^p[a_- - b_- p^2]\} \tag{A3a}$$

while with even p such that $m+2 \leqslant p \leqslant M-2$

$$C_{mp}=p(p^2-m^2)+\frac{1}{D_{ab}C_m}M(M^2-m^2)\{[a_- - b_-(M-1)^2][a_+ + b_+ p^2]$$
$$+ [a_+ + b_+(M-1)^2](-1)^p[a_- - b_- p^2]\}; \tag{A.3b}$$

again, $B_{mn}(R)$ is the boundary term given by

$$B_{mn}(R)= -\frac{1}{D_{ab}C_m}M(M^2-m^2)$$
$$\times\{[a_- - b_-(M-1)^2]g_{+n} + [a_+ + b_+(M-1)^2]\, g_{+n}\}. \tag{A.4}$$

The C_m in the above equations and the C_n in the equations to follow assume a value of 2 for m (or n) $=0$, and a value of 1 for m (or n) >0. The D_{ab} in Eqs. (A.1) to (A.4) is given by

$$D_{ab}= -\{[a_- - b_-(M-1)^2][a_+ + b_+ M^2] + [a_+ + b_+(M-1)^2][a_- - b_- M^2]\}. \tag{A.5}$$

The γ_{nq} and the $D_{mn}(R)$ in Eq. (2.12) are given as follows: for odd n with all q such that $0 \leqslant q \leqslant n+1$ and even q such that $n+3 \leqslant q \leqslant N-2$

$$\gamma_{nq}=\frac{1}{D_{AB}C_n}(N-1)[(N-1)^2-n^2]\{[A_- - B_- N^2][A_+ + B_+ q^2]$$
$$- [A_+ + B_+ N^2](-1)^q[A_- - B_- q^2]\}, \tag{A.6a}$$

while with odd q such that $n+2q \leqslant N-3$

$$\gamma_{nq}=\frac{1}{C_n}q(q^2-n^2)+\frac{1}{D_{AB}C_n}(N-1)[(N-1)^2-n^2]\{(A_- - B_- N^2)(A_+ + B_+ q^2)$$
$$- (A_+ + B_+ N^2)(-1)^q(A_- - B_- q^2)\}. \tag{A.6b}$$

$D_{mn}(R)$ is again the boundary term given by

$$D_{mn}(R)=\frac{1}{D_{AB}C_n}(N-1)[(N-1)^2-n^2]$$
$$\times\{[A_+ + B_+N^2]\,h_{-m}(R)-[A_- - B_-N^2]\,h_{+m}(R)\} \quad \text{(A.7)}$$

and for even n with all q such that $0\leqslant q\leqslant n+1$ and with odd q such that $n+3\leqslant q\leqslant N-2$

$$\gamma_{nq}=\frac{1}{D_{AB}C_n}N(N^2-n^2)\{[A_- - B_-(N-1)^2][A_+ + B_+q^2]$$
$$+\,[A_+ + B_+(N-1)^2](-1)^q[A_- - B_-q^2]\} \quad \text{(A.8a)}$$

while for q even such that $n+2\leqslant q\leqslant N-2$

$$\gamma_{nq}=\frac{1}{C_n}q(q^2-n^2)+\frac{1}{D_{AB}C_n}N(N^2-n^2)\{[A_- - B_-(N-1)^2][A_+ + B_+q^2]$$
$$\cdot\,[A_+ + B_+(N-1)^2](-1)^q[A_- - B_-q^2]\}. \quad \text{(A.8b)}$$

The boundary term $D_{mn}(R)$ is given by

$$D_{mn}(R)=-\frac{1}{D_{AB}C_n}N(N^2-n^2)$$
$$\times\{[A_- - B_-(N-1)^2]\,h_{+m}(R)+[A_+ + B_+(N-1)^2]\,h_{-m}(R)\}. \quad \text{(A.9)}$$

The D_{AB} in Eqs. (A.5)–(A.8) is given by

$$D_{AB}=-\{[A_- - B_-(N-1)^2][A_+ + B_+N^2]$$
$$+\,[A_- - B_-N^2][A_+ + B_+(N-1)^2]\}. \quad \text{(A.10)}$$

The P_i, $\hat{T}_{mn}$, Q_i, and $\hat{V}_{mn}$ in Eq. (3.8) are given by

$$P_i=\frac{1}{D_{\alpha\beta}}\{(\alpha_- + \beta_-d^{*(1)}_{LL})\,\beta_+d^{*(1)}_{0i}-(\beta_+d^{*(1)}_{0L})(\beta_-d^{*(1)}_{Li})\} \quad \text{(A.11a)}$$

$$\hat{T}_{mn}=\frac{1}{D_{\alpha\beta}}\{\beta_+d^{*(1)}_{0L}\hat{f}_{-mn}(\alpha_- + \beta_-d^{*(1)}_{LL})\,\hat{f}_{+mn} \quad \text{(A.11b)}$$

$$Q_i=\frac{1}{D_{\alpha\beta}}\{(\alpha_+ + \beta_+d^{*(1)}_{00})(\beta_-d^{*(1)}_{Li})-(\beta_-d^{*(1)}_{L0})(\beta_+d^{*(1)}_{0i})\} \quad \text{(A.11c)}$$

$$\hat{V}_{mn}=\frac{1}{D_{\alpha\beta}}\{(\beta_-d^{*(1)}_{L0})\,\hat{f}_{+mn}-(\alpha_+ + \beta_+d^{*(1)}_{00})\,\hat{f}_{-mn}\} \quad \text{(A.11d)}$$

where

$$D_{\alpha\beta} = \beta_+ \beta_- d_{L0}^{*(1)} d_{0L}^{*(1)} - (\alpha_- + \beta_- d_{LL}^{*(1)})(\alpha_+ + \beta_+ d_{00}^{*(1)}). \tag{A.12}$$

$\hat{f}_{+mn}$ and $\hat{f}_{-mn}$ are obtained from f_{+mn} and f_{-mn} via matrix operations described in Eqs. (3.3) and (3.4).

ACKNOWLEDGMENTS

The author is grateful to Professor S. Orszag of MIT, Dr. M. Deville of Université Catholique de Louvain, Professor A. Patera of MIT, and Dr. D. Haidvogel of NCAR for useful discussions. This work was supported by the Air Force Office of Scientific Research under Contract F49620-82-K-0002, Dr. J. D. Wilson, Program Manager.

REFERENCES

1. D. GOTTLIEB AND S. A. ORSZAG, "Numerical Analysis of Spectral Methods: Theory, and Application," SIAM, Philadelphia, 1977.
2. S. A. ORSZAG, *J. Comput. Phys.* **37** (1980), 70.
3. D. B. HAIDVOGEL AND T. ZANG, *J. Comput. Phys.* **30** (1979).
4. M. DEVILLE, paper presented at the Symposium on Spectral Methods for Partial Differential Equations, August 16–18, 1982, ICASE, NASA Langley Research Center, Hampton, Va.; Proceedings to be published by SIAM, Philadelphia.
5. T. A. ZANG, Y. S. WONG, AND M. Y. HUSSAINI, *J. Comput. Phys.* **48** (1982), 485.
6. D. GOTTLIEB, "The Stability of Pseudospectral-Chebyshev Methods," ICASE Rep. 79–17, Aug.10, 1979.
7. A. T. PATERA AND S. A. ORSZAG, *J. Fluid Mech.* **112** (1981), 467.
8. J. W. COOOLEY, P. A. W. LEWIS, AND P. D. WELCH, *J. Sound Vibration* **12**, No. 3 (1970), 315–337.